Unexpected Shortening of the Excited State Lifetime of Oxybenzone Radical Cation upon Excitation of the Band Origin

Juan C. Latorre,[1,2,3] Franco L. Molina,[1,2,3,4] Satchin Soorkia,[4] Michel Broquier,[4] Gilles Grégoire[4] and Gustavo A. Pino[1,2,3]**

SUPPLEMENTARY INFORMATION

Table S1: Relative energy, including the zero point energy correction (ZPE) for the different isomers optimized at the DFT level with the CAM-B3LYP functional and the aug-cc-pVDZ basis set.

Isomer	Relative Energy + ZPE (eV)	Relative Energy + ZPE (cm^{-1})
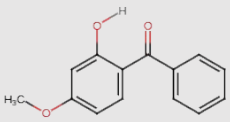 ENOL-IN-UP	0	0
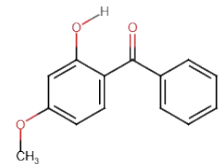 ENOL-IN-DOWN	0.159	1282
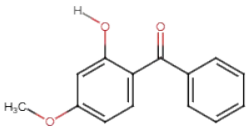 ENOL-OUT-UP	0.387	3122
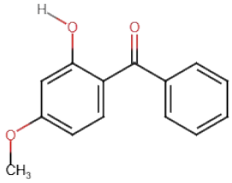 ENOL-OUT-DOWN	0.45	3630
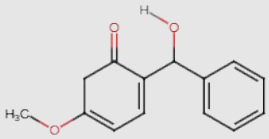 KETO-UP	0.031	250
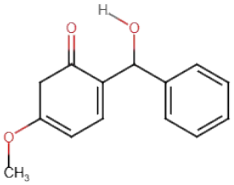 KETO-DOWN	0.110	887

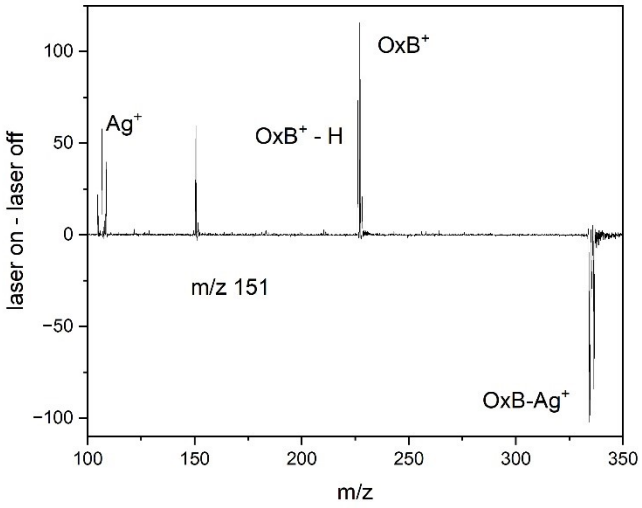

Figure S1: Difference (laser on – laser off) Photo Dissociation Mass Spectrum (PD-MS) of OxB-Ag^+ taken at 310 nm.

Assignment of the experimental spectrum

To assign the experimental spectrum, vertical excitation energies (E_v) and oscillator strengths (OS) were calculated for the first eight excited states of both tautomers and are reported in Table SI2.

Special care was taken to follow the same electronic state along the optimization. The dominant orbital transitions were monitored at each step, and the excitation character was verified for continuity.

The adiabatic excitation energies (E_{ad}) including the ZPE difference (ΔZPE) between the D_0 and the D_n excited state were also calculated for the enol tautomer (Table SI2) (all reported values are shown in Figure 3). It should be noted that for the keto tautomer, optimizations for all excited states led to barrierless H^+ transfer, thus forming the enol tautomer. This suggests that the keto tautomer is unstable in the excited states.

Table S2: Vertical (E_v) and adiabatic (E_{ad}) excitation energies (in eV), including ΔZPE correction, and Oscillator Strengths (OS) of the first eight excited states of the Enol and Keto tautomers of $OxB^{\bullet+}$. The relative energy of both tautomers in the ground state (D_0) are shown in parenthesis. For the Enol tautomer E_{ad} was calculated only for those excited states whose E_v are above the experimental 0_0^0 transition. For the Keto tautomer, the D_0 state is the only stable state, all excited states undergo proton transfer to form the enol tautomer.

	Enol (0.00 eV)			**Keto** (0.031 eV)	
	E_v (eV)	E_{ad} (eV)	OS	E_v (eV)	OS
D_1	1.20	-	0.0029	1.24	0.0148
D_2	1.74	-	0.0084	1.80	0.0004
D_3	1.95	-	0.0049	2.38	0.0314
D_4	2.02	-	0.0058	2.47	0.0037
D_5	2.98	2.71	0.0615	3.15	0.0363
D_6	3.20	2.68	0.0025	3.35	0.1021
D_7	3.76	3.48	0.0003	3.66	0.0021
D_8	3.91	3.54	0.0012	3.74	0.0382

E_{ad} of the $D_0 \rightarrow D_5$ or $D_0 \rightarrow D_6$ transitions of the enol tautomer, whose orbitals are shown in Figure S2, are calculated close to the experimental 0_0^0 transition. The experimental spectrum can be confidently assigned to the $D_0 \rightarrow D_5$ transition because of its larger

oscillator strength (30 times larger than $D_0 \rightarrow D_6$ transition) and much better agreement of the simulated Franck-Condon spectrum with the experimental spectrum. The simulated FC spectrum for the $D_0 \rightarrow D_5$ and $D_0 \rightarrow D_6$ transitions are compared to the experimental PD spectrum in Figure S3. The FC spectrum has been calculated for a temperature of 20 K and convoluted by a Gaussian function of 10 cm^{-1} to take into account the laser linewidth. The $D_0 \rightarrow D_6$ spectrum is three orders of magnitude less intense than the $D_0 \rightarrow D_5$ spectrum and with very low FC factors near the 0_0^0 transition. This is due to the large geometry change between D_0 and D_6. In particular, the $O_2H_1O_6C_5$ dihedral angle deviates significantly from planarity, changing from ~7° in the D_0 and D_5 states to ~23 ° in D_6. Furthermore, the dihedral angle $O_6C_5C_7C_8$ changes from ~ -30° to ~ -15° between the D_0 and the D_6 states. The main structural changes are reported in Table SI3. Overall, the position of the vibronic transitions is reproduced satisfyingly by the spectrum corresponding to the $D_0 \rightarrow D_5$ transition, but the bandwidths are underestimated, particularly for the band origin.

Table S3: Relevant geometric dihedral angles (°) and bond distances (Å) in the optimized structures of the D_0, D_5 and D_6 states of $OxB^{\bullet+}$.

Geometrical Parameters (° / Å)	**D_0 Optimized Structure**	**D_5 Optimized Structure**	**D_6 Optimized Structure**
$O(2)H(1)\hat{O}(6)C(5)$	-6.72	-6.76	-23.23
$C(3)C(4)\hat{C}(5)O(6)$	-15.8	-9.4	-31
$O(6)C(5)\hat{C}(7)C(8)$	-30.1	-32.8	-14.6
$O(4)C(5)\hat{8}C(7)C(8)$	148.8	147.5	167.1
$R(O2-H1)$	1.020	1.008	0.993
$R(O6-H1)$	1.533	1.589	1.702

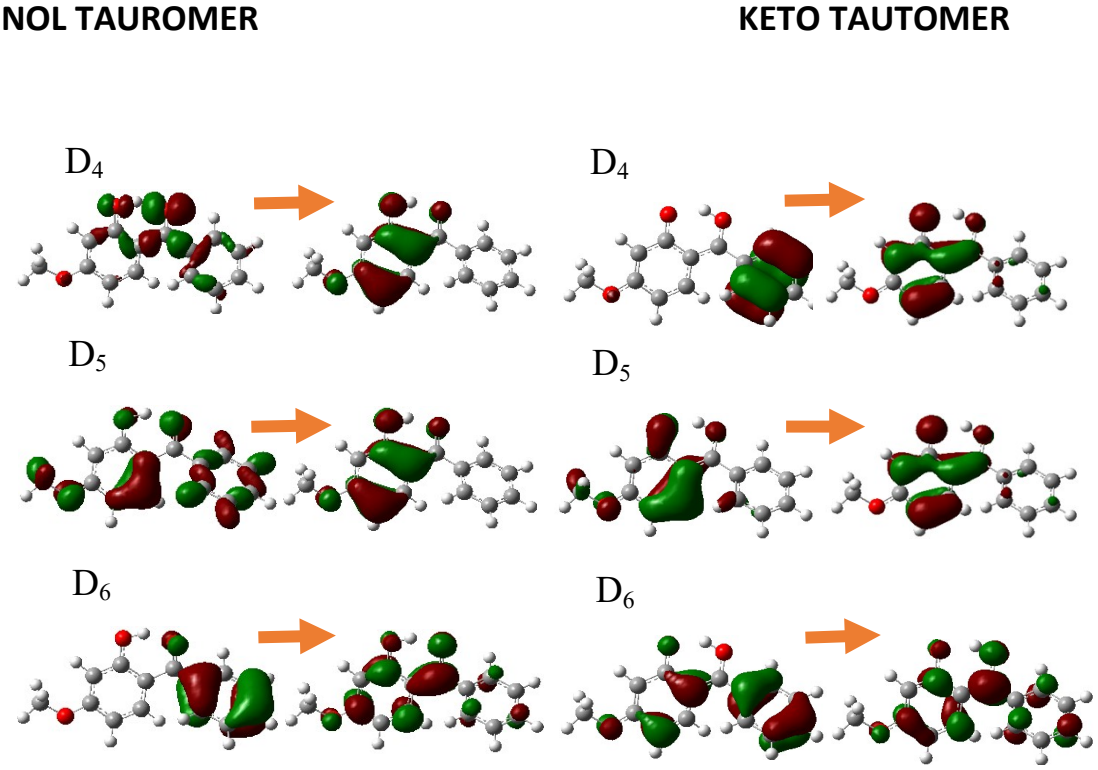

Figure S2: Molecular Orbitals involved in the D_4, D_5 and D_6 states of the enol (left) and keto (right) tautomers, using an iso value of 0.06.

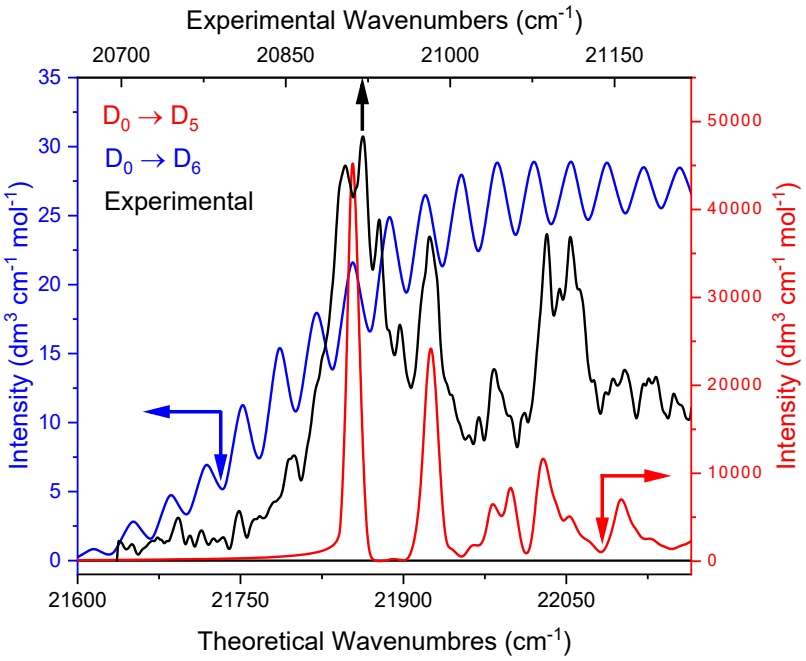

Figure S3: Experimental (black) and calculated spectra for the $D_0 \rightarrow D_5$ (red) and $D_0 \rightarrow D_6$ (blue) transitions, convoluted to Gaussian functions with FWHM = 10 cm^{-1} and T = 20 K. The arrows indicate the axis and scale for each spectrum (in the same color code). Note the different intensity scales for the $D_0 \rightarrow D_5$ and $D_0 \rightarrow D_6$ transitions.

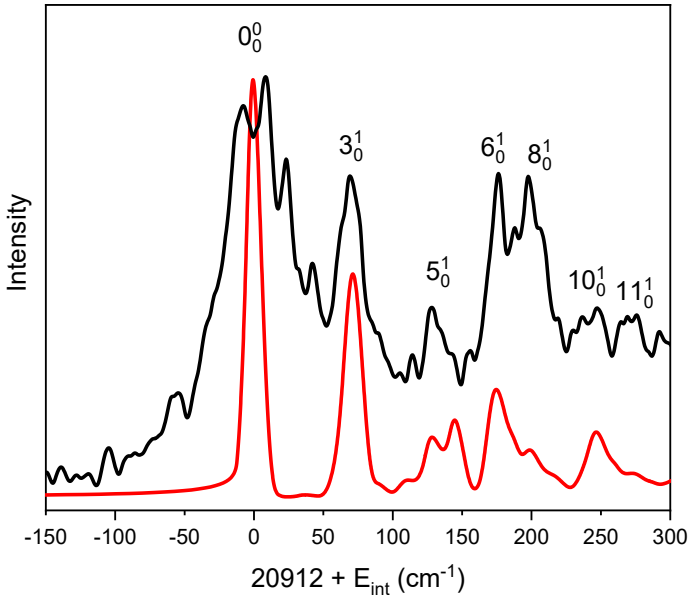

Figure S4: Vibrational assignment based on the Franck-Condon simulation for the for the $D_0 \rightarrow D_5$ transition.